



ISSN: 0067-2904

## Study of Land Cover Changes of Baghdad Using Multi-Temporal Landsat Satellite Images

Bushra Q. Al-Abudi<sup>1</sup>, Mohammed S. Mahdi<sup>2</sup>, Yasser Chasab Bukheet<sup>1\*</sup>

<sup>1</sup>Astronomy and Space Department, College of Science, Baghdad University, Baghdad, Iraq

<sup>2</sup>Computer Science Department, College of Science, Al-Nahrain University, Baghdad, Iraq

### Abstract

The main goal of this work is study the land cover changes for "Baghdad city" over a period of (30) years using multi-temporal Landsat satellite images (TM, ETM+ and OLI) acquired in 1984, 2000, and 2015 respectively. In this work, The principal components analysis transform has been utilized as multi operators, (i.e. enhancement, compressor, and temporal change detector). Since most of the image band's information are presented in the first PCs image. Then, the PC1 image for all three years is partitioned into variable sized blocks using quad tree technique. Several different methods of classification have been used to classify Landsat satellite images; these are, proposed method singular value decomposition (SVD) using Visual Basic software and supervised method (Maximum likelihood Classifier) using ENVI 5.1 software are utilized in order to get the most accurate results and then compare the results of each method and calculate the land cover changes that have been taken place in years 2000 and 2015; comparing with 1984. The image classification of the study area resulted into five land cover types: Water body, vegetation, open land (Barren land), urban area "Residential I" and urban area "Residential II". The results from classification process indicated that water body, vegetation, open land and the urban area "Residential I" are increased, while the second type from urban area "Residential II" in decrease to year 2015 comparable with 1984. Despite use of many methods of classification, results of the proposed method proved its efficiency, where the classification accuracies for the (SVD) method are 81%, 78% and 80% for years 1984, 2000 and 2015 respectively.

**Keywords:** Landsat satellite images, land cover change detection, singular value decomposition

### دراسة التغيرات بالغطاء الارضي لمدينة بغداد بأستخدام صور القمر الصناعي لاندسات

بشرى قاسم العبودي<sup>1</sup>، محمد صاحب مهدي<sup>2</sup>، ياسر جاسب بخيت<sup>1\*</sup>

<sup>1</sup>قسم الفلك والفضاء، كلية العلوم، جامعة بغداد، بغداد، العراق

<sup>2</sup>قسم الحاسبات، كلية العلوم، جامعة النهرين، بغداد، العراق

### الخلاصة

ان الهدف الرئيسي من هذا العمل، هو دراسة التغيرات بالغطاء الارضي لمدينة بغداد خلال فترة زمنية تمتد لأكثر من (30) سنة بأستخدام صور القمر الصناعي لاندسات ( TM, ETM+, OLI ) للاعوام 1984، 2000 و 2015 على التوالي. في هذا العمل استُخدم تحويل ( principal components analysis transform ) كعامل تحويل ذو فوائد متعددة لاغراض (تحسين الصورة الفضائية، ضغط بيانات الصورة الفضائية وكشف التغيرات الزمنية) لتوليد صورة جديدة متكاملة ذات معلومات كثيفة مركزة وتباين أفضل وذلك بتجميع معلومات كل الحزم المختلفة في الصورة المتكاملة (PC1 image). بعد ذلك تم تجزئة الصورة

\*Email: yassermobark377@gmail.com

المتكاملة الى اجزاء صغيرة ومتغيرة الحجم بأستخدام تقنية التقسيم الشجري الرباعي. ان حجم جزء الصورة يحدد ذاتياً طبقاً الى مقاييس الانتظامية الطيفية. تم أستخدام اكثر من طريقة لغرض تصنيف صور القمر الصناعي لاندسات لمنطقة الدراسة منها، الطريقة المقترحة وهي خوارزمية تحليل القيمة المنفردة (SVD) بأستخدام برنامج (Microsoft Visual Basic Software)، وكذلك طريقة التصنيف المراقب (Maximum Likelihood Classifier) بأستخدام برنامج (ENVI 5.1 software) وذلك للحصول على أدق النتائج ومن ثم مقارنة نتائج هذه الطرق وحساب التغييرات بالغطاء الارضي التي حدثت في سنة 2000 وسنة 2015 بالمقارنة مع سنة 1984. ان نتائج التصنيف للطرق المستخدمة لمنطقة الدراسة افضت الى خمسة انواع من الغطاء الارضي هي مساحات مائية، مناطق خضراء، مناطق مفتوحة (مناطق غير مثمرة)، مناطق سكنية نوع أول (عالية الكثافة) ومناطق سكنية نوع ثاني (متوسطة الكثافة). أشارت النتائج النهائية أن المساحات المائية والمناطق الخضراء والاراضي المفتوحة والنوع الأول من المناطق السكنية في حالة زيادة بينما النوع الثاني من المناطق السكنية في حالة تناقص خلال السنوات من 1984 الى 2015. على الرغم من استخدام اكثر من طريقة للتصنيف أثبتت نتائج الطريقة المقترحة كفاءتها ومقبوليتها بالمقارنة مع طريقة (Maximum Likelihood method) حيث كانت دقة التصنيف للطريقة المقترحة (خوارزمية تحليل القيمة المنفردة) 81%، 78%، 80% للسنوات 1984، 2000 و 2015 على التوالي.

## 1. Introduction:

Remotely sensed imagery can be used in a number of applications. A principal application of remotely sensed data is to create a classification map of the identifiable or meaningful features or classes of land cover types in a scene [1]. Classification is one of the data mining methods, which are used to classify the object into predefined group. It is the most frequently used decision-making tasks of human activity. A classification problem occurs when an object needs to be assigned into a predefined group or class based on a number of observed attributes related to that object. The classification also plays very important role in the remote sensing and satellite image classification [2]. Image classification is a complex process that may be affected by many factors. Huge number of classification techniques can be found in the literature; mostly they have been categorized as either supervised or unsupervised methods. The supervised techniques are often required prior knowledge in selecting correct region of interest "ROI", inadequate selection of "ROI" or the number of correct existed regions, often, yields an inadequate classification result, while the unsupervised methods need to identify the correct number of regions existed in the processed image. Change detection is a process to measure the extent of the change in the characteristics of a particular area, and the disclosure of this change involves a comparison of aerial photographs or satellite images of the area taken at different time intervals to measure the urban development and environmental changes using two or more of the scenes that cover the same geographical area over two or more times [3]. In this paper, we classified Landsat satellite images of Baghdad city for years 1984, 2000 and 2015 using two software programming (Microsoft Visual Basic Program, 2012 and ENVI 5.1 software, 2013). Supervised classification methods have been used to classify satellite image; these were proposed supervised method (singular value decomposition) using Visual Basic software and supervised method (Maximum Likelihood Classifier) using ENVI 5.1 software.

## 2. Area of Study:

The study area is Baghdad city. It is the capital and the main administrative center of Iraq. Baghdad is located in the central part of Iraq on both sides of Tigris River with geographic coordinates: Latitude ( $33^{\circ}25'46''$ ) to ( $33^{\circ}24'21''$ ) N, Longitude ( $44^{\circ}15'55''$ ) to ( $44^{\circ}17'38''$ ) E. Baghdad is the largest and most heavily populated city in Iraq. Baghdad is suited in a plain area of an elevation between (31-39 m) above sea level. So, no natural boundaries exists that limits the aerial extension of the city. The Tigris River passes through the city dividing it into two parts; Karkh (Western part) and Rusafa (Eastern part). The area is bounded from the east by Diyala River, which joins the Tigris River southeast of Baghdad. The Army Canal, 24 km long, recharges from the Tigris River in the northern part of the city and terminates in the southern part of Diyala River. Figure-1 shows the study area "Baghdad city" for period 1984, 2000 and 2015.

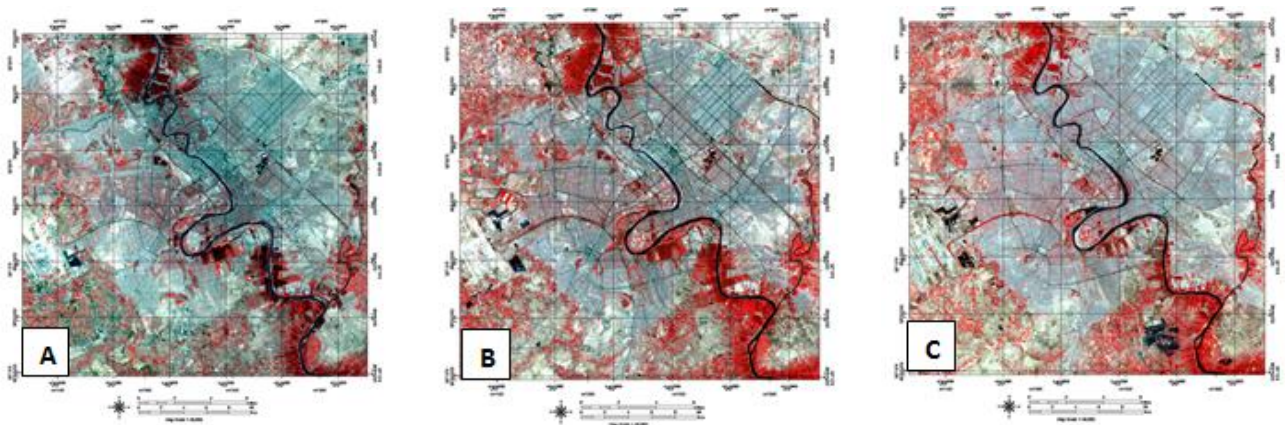


**Figure 1-** Area of study "Baghdad city"

(A) Landsat- 5 (TM) satellite image (1984), false color composite (Band 4, Band 3, Band 2)

(B) Landsat- 7 (ETM+) satellite image (2000), false color composite (Band 4, Band 3, Band 2)

(C) Landsat- 8(OLI) satellite image (2015), false color composite (Band 5, Band 4, Band 3)

### 3. Satellite Image Pre-Processing:

Generally, raw satellite image contain some errors and will not be directly utilized for features identification and any applications. It needs some correction. Pre-processing is done before the main data analysis and extraction of information. Pre-processing involves two major processes: geometric correction and radiometric correction or haze correction. [4]. In this paper, ENVI 5.1 software was used to perform most satellite image pre-processing stages.

#### 3.1 Importing of Landsat Images:

In this stage, all downloaded Landsat TM, ETM+ and OLI satellite images for years 1984, 2000 and 2015 were unzipped and imported to ENVI 5.1 software environment. Then all the bands of each satellite image were gathered together in a single layer "layer stacks" or "multiband images" using the layer-stack function of ENVI 5.1 software and saved with ENVI format. Bands 1 to 5 and band 7 were utilized for the Landsat TM and ETM+ images. While, bands 2 to 6 and band 7 were utilized for the Landsat OLI images. Bands 1 to 4 are categorized as the visible bands (Blue band, Green band, Red band) or the near Infrared (NIR) band. Meanwhile bands 5 and 7 are considered the short wave infrared bands.

#### 3.2 Geometric Correction:

Geometric correction of the data is critical step for performing a change detection analysis [4]. In this work, the geometric correction of the satellite data has not been performed; all satellite images obtained from the ("<http://earthexplorer.usgs.gov/>") site were geo-registered to the same Universal Transversal Mercator (WGS\_1984\_UTM\_Zone\_38N) coordinate system. Subsequently, all satellite images (Landsat-5 TM 1984, Landsat-7 ETM+ 2000 and Landsat-8 OLI 2015) carried out according to WGS\_84 datum and UTM\_Zone\_38N projection, using nearest neighbor re-sampling method.

#### 3.3 Radiometric and Atmospheric Correction:

Since digital sensors record the intensity of electromagnetic radiation from each spot viewed on the Earth's surface as a Digital Number (DN) for each spectral band, the exact range of DN that a sensor utilizes depends on its radiometric resolution [5]. Therefore, normalizing image pixel values for differences in sun illumination geometry, atmospheric effects and instrument calibration is necessary specially because a time series of Landsat imageries will be used, from 1984 to 2015 (TM, ETM+ and OLI), and compared to each other. The radiometric correction was used to restore the image by using sensor calibration concerned with ensuring uniformity of output across the face of the image, and across time. ENVI 5.1 software has been used to perform the radiometric correction and atmospheric correction using "Radiometric Correction Tools" and "Dark Object Subtraction Tools" respectively.

#### 3.4 Clipping the Area of Study:

The study area "Baghdad city" locates in center of Iraq with the following geographic coordinate: ULX (44°13' W), LRX (44°32' E), ULY (33°26' N) and LRY (33°10' S). The image is clipped to the rectangular boundary "square size" of the study area. The clipped image consists of 1024 columns and 1024 rows. All images were secured to have the same number of rows and columns. This step is performed using subset data with region of interest (ROIs) tools in ENVI 5.1 software.

**4. Proposed Classification Method:**

The proposed classification method includes three main stages: The principle component analysis (PCA) transform is first employed to create newly integrated image with dense information and best contrast due to the information of all used bands are concentrated in one image (PC1 image). Then, the PC1 image is segmented into variable sized blocks using quad tree partitioning method. Later stage, the singular value decomposition method (SVD) is adopted to perform the supervised classification that classifies the study area and obtains the members of each class. Figure-2 illustrate the block diagram of the proposed classification method. More details for each step can be shown in following subsections.

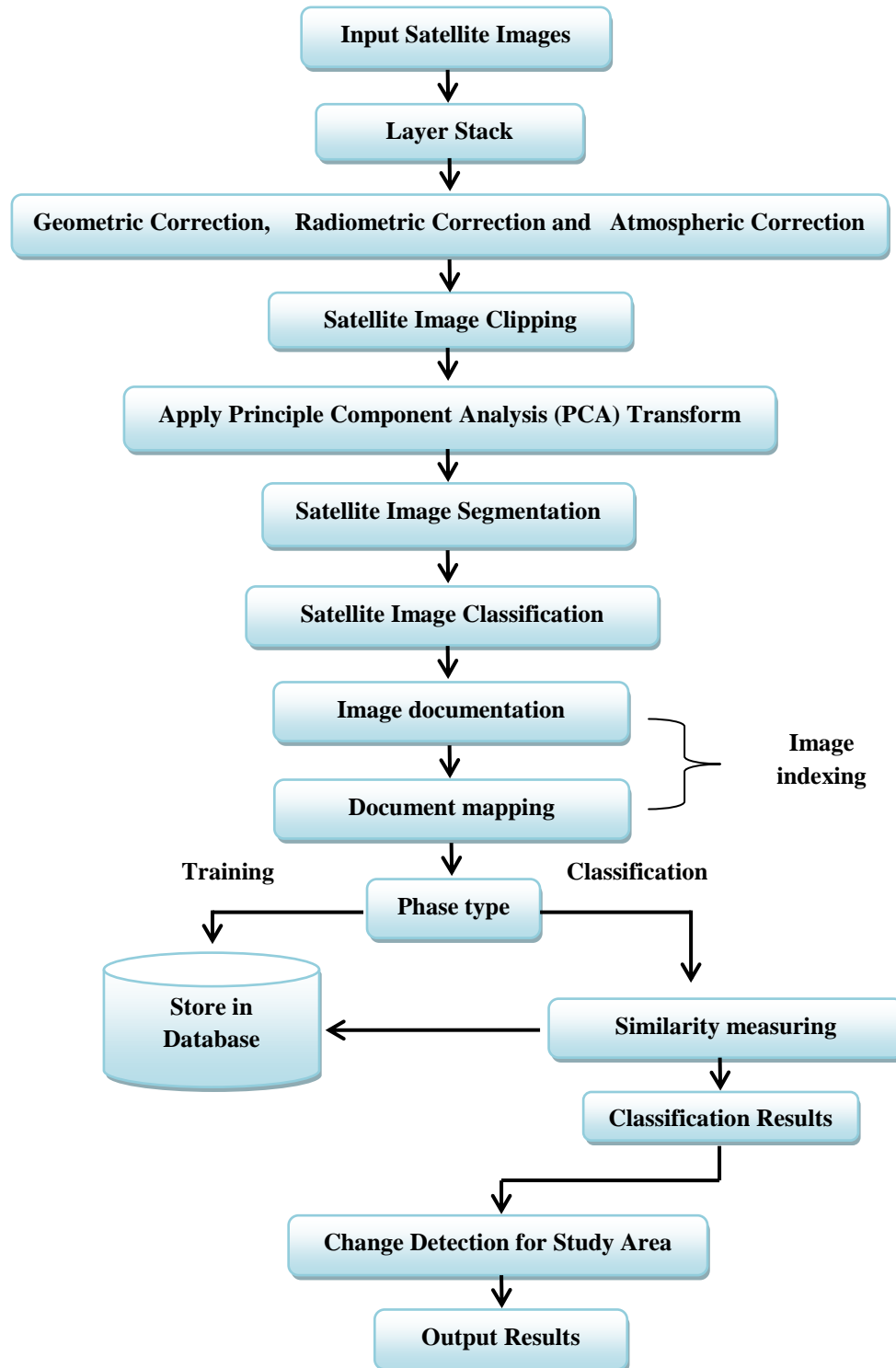


Figure 2- Block Diagram of the proposed classification method



#### 4.1 Principal Component Analysis Transform:

The main idea of principal components analysis (PCA) transform is to reduce the dimensionality of a set of bands, which contains numerous interconnected variables. The PCA algorithm transforms those variables into a new set of decorrelated ones. The order of new variables is such that usually only the first few are responsible for most of the variances in the original bands. PCA transform uses the input image bands to create new principles components (PCs). The newly images will have characteristics of dense information and best contrast. Therefore, the first principle component is suitable for classifying the multiband satellite images [6,7].

The principal components analysis of KL-transform has been utilized as multi operators, (i.e. enhancement, compressor, and temporal change detector). Since most of the image band's information are presented in the first PCs, therefore image classification and change detection procedures are performed with little consuming time. The linear "PCA" transformation can be used to translate and rotate data into a new coordinate system that maximizes the variance of the data. It can also be implemented for enhancing the information content . In this section, and after achievement satellite image pre-processing stages, we will be perform PCA transform on the Landsat images of study area for years 1984, 2000 and 2015 using proposed system (See Figure-3).

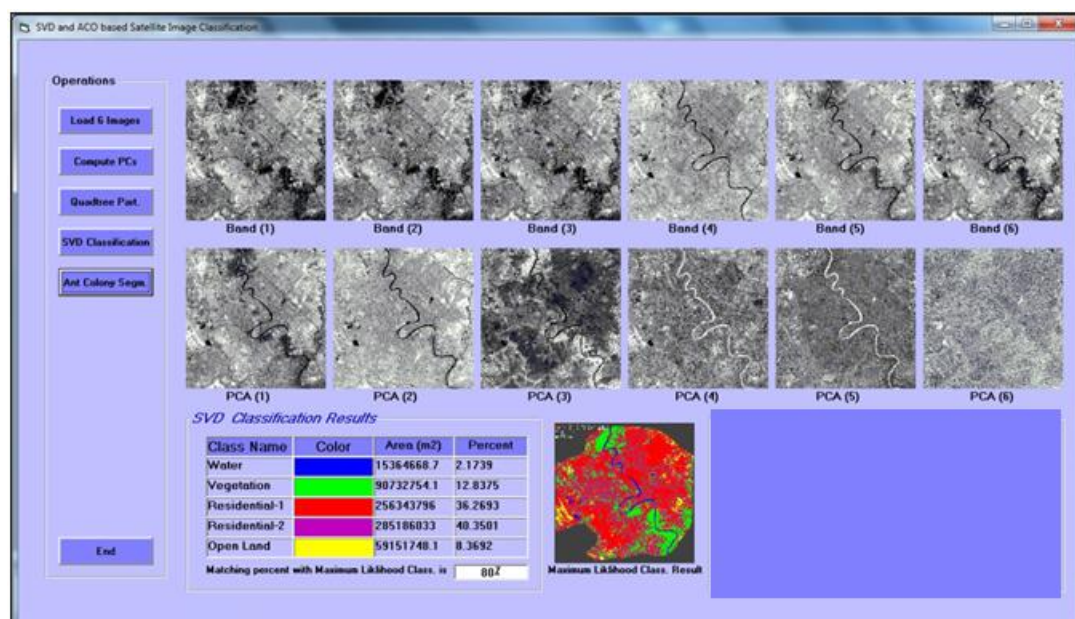
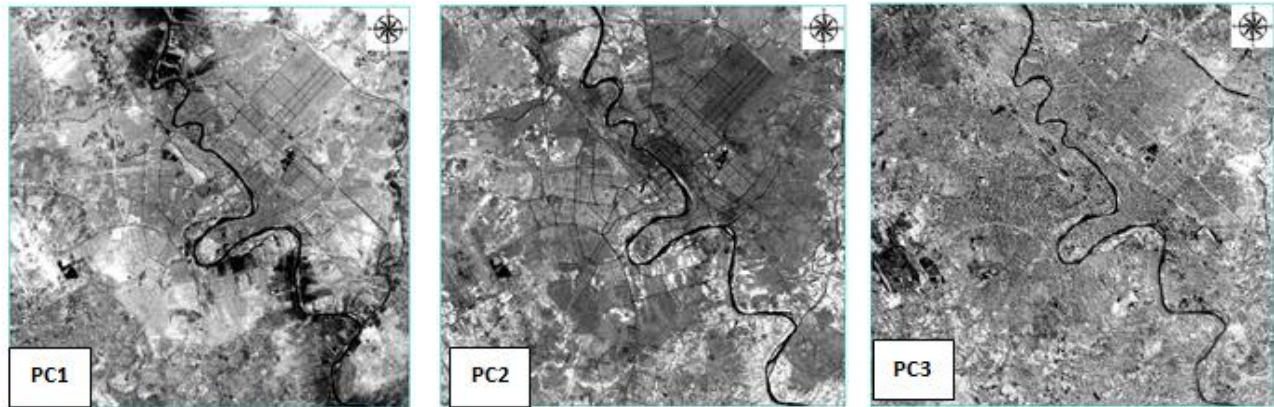
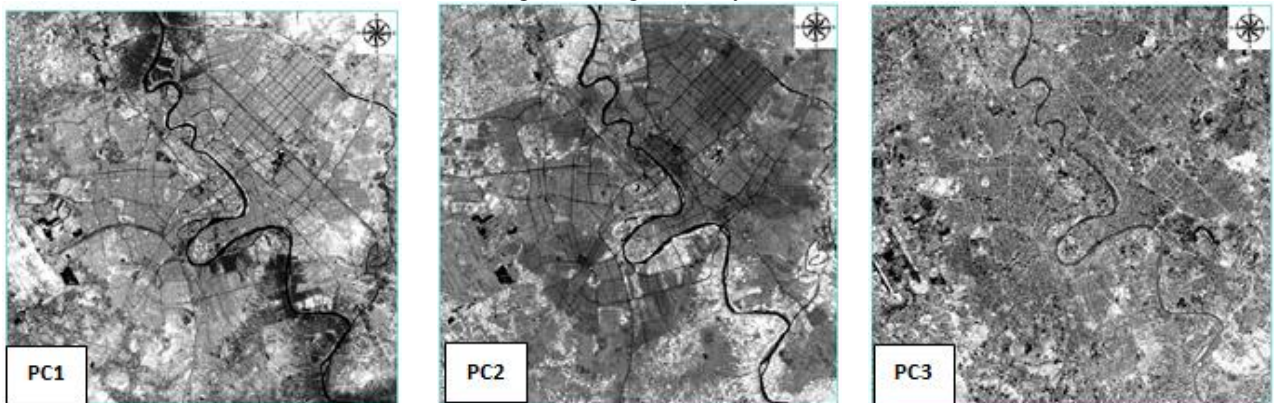


Figure 3- Proposed System Interface

In our work, the PCA transform is applied to transform six multibands 1, 2, 3, 4, 5 and 7 of Landsat TM, ETM+ images and six multibands (2, 3, 4, 5, 6 and 7) of Landsat-8 OLI images to six principal component images. Only first PCA was chosen because it has higher potential information. The higher potential image is indicated by its PCA eigenvalue. The higher eigenvalue shows higher variance in the image, which means that the image has (lower data redundancy) and a PCA transformation is done by transforming each image into a new PCA image. Although six components are generated from the original bands, PCA1 is responsible for more than 95% of the total variation for each satellite image. It is provide the most information about different ground features. The first PC layer shows 95.8387%, 96.2976% and 99.1282% of the total variance for 1984, 2000 and 2015 Landsat images respectively. The first PC contains the most ground information and can be used to compare the changes in land cover classes in different years for the study area. The PC1, PC2 and PC3 layers for the 1984, 2000 and 2015 images is shown in Figures-4, 5 and 6 respectively.



**Figure 4-** Results of PCA Transform Generated from Bands of Landsat-5 (TM) Satellite Images for Baghdad City (27/8/1984)



**Figure 5-** Results of PCA Transform Generated from Bands of Landsat-7 (ETM+) Satellite Images for Baghdad City (31/8/2000)

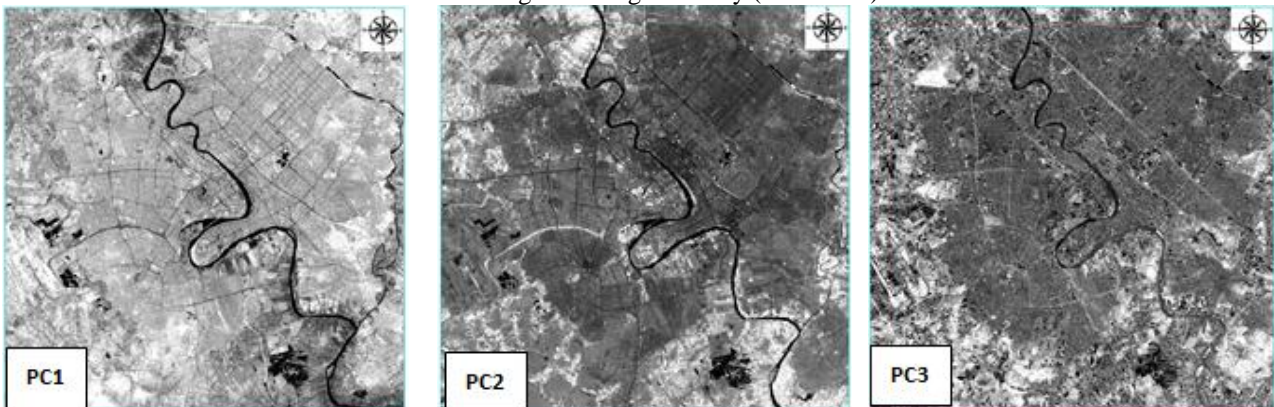


**Figure 6-** Results of PCA Transform Generated from Bands of Landsat-8 (OLI) Satellite Images for Baghdad City (1/8/2015)

#### 4.2 Satellite Image Segmentation:

One of the most familiar partition techniques is the quad tree method, which subdivides a region of an image into four equal blocks when a given homogeneity criterion is not met by that region. It continues to divide each sub-division until the criteria is met or minimum block size is reached. Typically, an image is initially divided into a set of large blocks (their size equal to the maximum allowable block size). The variance is computed and compared to a threshold for each of these blocks. Any sub-blocks created by failure of the homogeneity test undergo the same procedure. The subdivision will continue until a block either reaches a minimum size or it satisfies the homogeneity criterion. Each block test constitutes a node of the quad tree. A node for which no further subdivision is needed is called a leaf [8]. In this work, a quad tree algorithm is proposed; it is based on the image uniformity criterion. In this section, we applied quad tree algorithm to partition the first principle component (PCA 1) image for years 1984, 2000 and 2015 into sub regions represents the area of study. The efficiency of such method is due to its ability to effectively partitioning diversity regions in

the satellite image. Satellite image segmentation algorithm can be given in algorithm (1) as the following [8]:

**Algorithm (1): Satellite Image Segmentation using Quad tree Algorithm**

**Input:**

*PcImg*: first PCA image band

*Wdth*: width of the first PC image

*Hght*: height of the first PC image

**Output:**

*Llist*: One-dimensional array represents grid of quad tree partitioning

**Procedure:**

**Step 1:** Compute the global mean ( $M$ ) and the standard deviation ( $\sigma$ ) of the whole input (initial) image, this factor will be used to automatically determine the threshold value of the dispersion level (in the uniformity criterion).

**Step 2:** Set the values of some partitioning control parameters, which can be considered as attributes of the partitioning process, these parameters are the:

- A. Maximum block size ( $S_{max}$ ): represent the maximum size of the block corresponds to the minimum depth of the tree partitioning.
- B. Minimum block size ( $S_{min}$ ): represent the minimum size of the block corresponds to the maximum depth of the tree partitioning.
- C. Inclusion factor ( $\alpha$ ): represent the multiple factor, when it is multiplied by the global standard deviation ( $\sigma$ ) it will define the value of the extended standard deviation ( $\sigma_e$ ), i.e.  $\sigma_e = \alpha\sigma$ .

- D. Acceptance Ratio (R): represent the ratio of the number of pixels whose values differ from the block mean by a distance more than the expected extended standard deviation.

**Step 3:** In order to store information about quad tree partitioning process, quad tree link list was utilized, it is defined as an array of records, each record of type quad tree link list consist of the following parameters:

- i. Position: represented by the  $X$  and  $Y$  coordinates of the upper left corner of each block
- ii. Size: represent the size of each image block, which is equal either to width or height of the image block, since in quad tree the blocks have square shape
- iii. Next: it is a pointer to the next block in the quad tree

**Step 4:** The segmentation process by quad tree algorithm start with partitioning the image into blocks whose size is equal to the maximum allowable block size.

**Step 5:** Check the uniformity criteria for each sub-block as follows:

- A. Compute the local mean of the sub-block ( $m$ ).
- B. Compute number of undesired pixels within the sub-block ( $N_p$ ), which may differ from the absolute value of mean ( $m$ ) and pixel value  $f(x, y)$  by a distance more than ( $\sigma_e$ ), those pixels satisfy the condition

$$|f(x, y) - m| > \sigma_e, \quad \text{Where, } f(x, y) \text{ is the pixel value.}$$

- C. If the ratio of undesired pixels ( $N_p/S$ ), where  $S$  is the block size, is less than the acceptance ratio then the block is considered uniform (i.e., don't partition), otherwise the block should be partitioned into four child sub-blocks (corresponding to create new four quad tree link list records). Each block should be examined by measuring its uniformity if it does not satisfy the uniformity criteria, then the partitioning is repeated until the uniformity condition is satisfied or the child block reach the minimum size. After completing the partitioning sequence, the constructed quad tree will consist of partitions whose size value will be between the minimum and maximum block size.

Figure-7 show the segmentation results using quad tree algorithm of the PCA1 image with different segmentation control parameters for Landsat-5 TM (27/8/1984) satellite image. It is observed that the sizes of the image blocks are variable. In all parts, the block size was automatically determined according to the details variety. The testing results had indicated that the used algorithm is a simple and powerful framework for the quad tree segmentation. The control parameters have different influence on the segmentation results. In our work, the best results were obtained when the control



parameters as the following: maximum block size=8, minimum block size=4, inclusion factor =0.5, acceptance ratio=0.1 and mean factor=0.05.

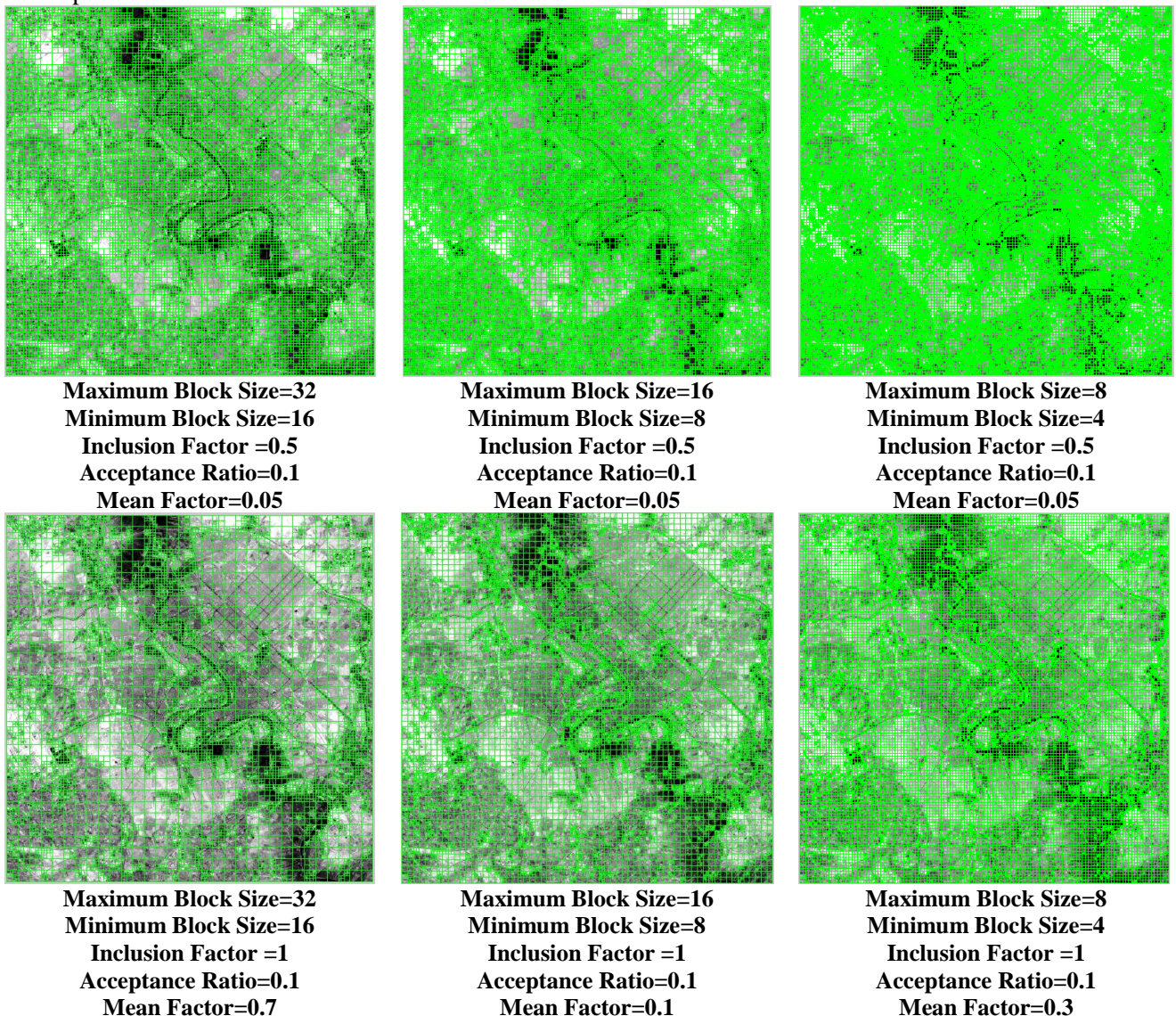


**Figure 7-** Results of quad tree segmentation applied on the PCA- 1 image generated from Landsat-5 (TM) satellite image (27/8/1984) with different partitioning control parameters

#### 4.3 Supervised Classification using SVD Algorithm:

Singular Value Decomposition (SVD) is a powerful tool in multispectral image analysis. The SVD of a matrix can be directly used for noise reduction, data compression, and dimension reduction. In addition, it is also related to the processes of classification. Latent semantic analysis is a vector space model for index and retrieval of information technology, this method mainly uses singular value decomposition (SVD) and reduces dimension as the basis of the theory of modules to find implicit concept in document. Some of the latent semantic analysis researches are used in text or web pages. SVD is a decomposition technology and uses the singular value decomposition to reduce the size of the high-dimensional matrix. Through dimension reduced, can extracted important information in the semantic space. After the decomposition, new matrix and original matrix of the features are similar and new matrix can more accurately describe the matrix of the hidden semantic concept [9-11].

In our work, we adopt singular value decomposition to selected important semantic features in scenes and classify the satellite image. Singular value decomposition (SVD) is proposed to perform supervised classification for partitioned PC1 image, it is consists of two phases: the training and classification. The training phase is responsible on storing the classes in the database file. The training area consists of five land cover classes (water, vegetation, open land, residential I and residential II),



training area are collected from all parts of the study area. While the task of classification phase is to compute the similarity measure between the SVD of the target image and SVD of the classes, found in the database. Satellite image classification algorithm using SVD can be given in algorithm (2) as the following:

**Algorithm (2): Satellite Image Classification using SVD Algorithm**

**Input:**

*PC Img*: two-dimensional array is the first *pc* image

*A*: 2D array represents the training data from image and vector *q* that represent the block from image embedded with *A*

*m*: the row dimension of *A*

*n*: the column dimension of *A*

**Output:**

*U*: an *m*-by-*n* orthogonal matrix represents the left singular value

*V*: an *n*-by-*n* orthogonal matrix represents the right singular value

*S*: an *n*-by-*n* diagonal matrix represents the left singular value

*ClasImg*: two-dimensional array represents the colored map of classification results

**Procedure:**

**Step 1:** Takes an *m*x*n* matrix *a* and decomposes it into *u**w**v*, where *u*, *v* are left and right orthogonal transformation matrices, and *d* is *a* diagonal matrix of singular values

**Step 2:** Input to svd is as follows:

i. *a* = *m*x*n* matrix to be decomposed, gets overwritten with *u*

ii. *m* = row dimension of *a*

iii. *n* = column dimension of *a*

iv. *w* = returns the vector of singular values of *a*

v. *v* = returns the right orthogonal transformation matrix.

**Step 3:** Apply Householder reduction to bidiagonal form to the left-hand reduction and to the right-hand reduction.

**Step 4:** Accumulate the right-hand transformation.

**Step 5:** Accumulate the left-hand transformation.

**Step 6:** Diagonalization of the bidiagonal form (Loop over singular value and over allowed iterations).

**Step 9:** Find the convergence by making singular value non-negative.

**Step 10:** Apply Shift from bottom 2 x 2 minor and compute the next *QR* transformation.

**Step 11:** Apply arbitrary rotation if singular value equal to zero.

**Step 12:** return *v* and *w*.

**Step 14:** Assign a specific color for each label, and draw the image (*ClasImg*) with the new coloring, which is the classified image.

In this method Landsat images at different time classified into five classes. These classes represent five major features in the study area (water, open land, vegetation, residential land I and residential land II). The results from applying singular value decomposition classification algorithm are shown in Figure-8 for Landsat (TM, ETM+ and OLI) satellite images. Table-1 shows the results of supervised classification statistics for all three years 1984, 2000 and 2015 using SVD algorithm.

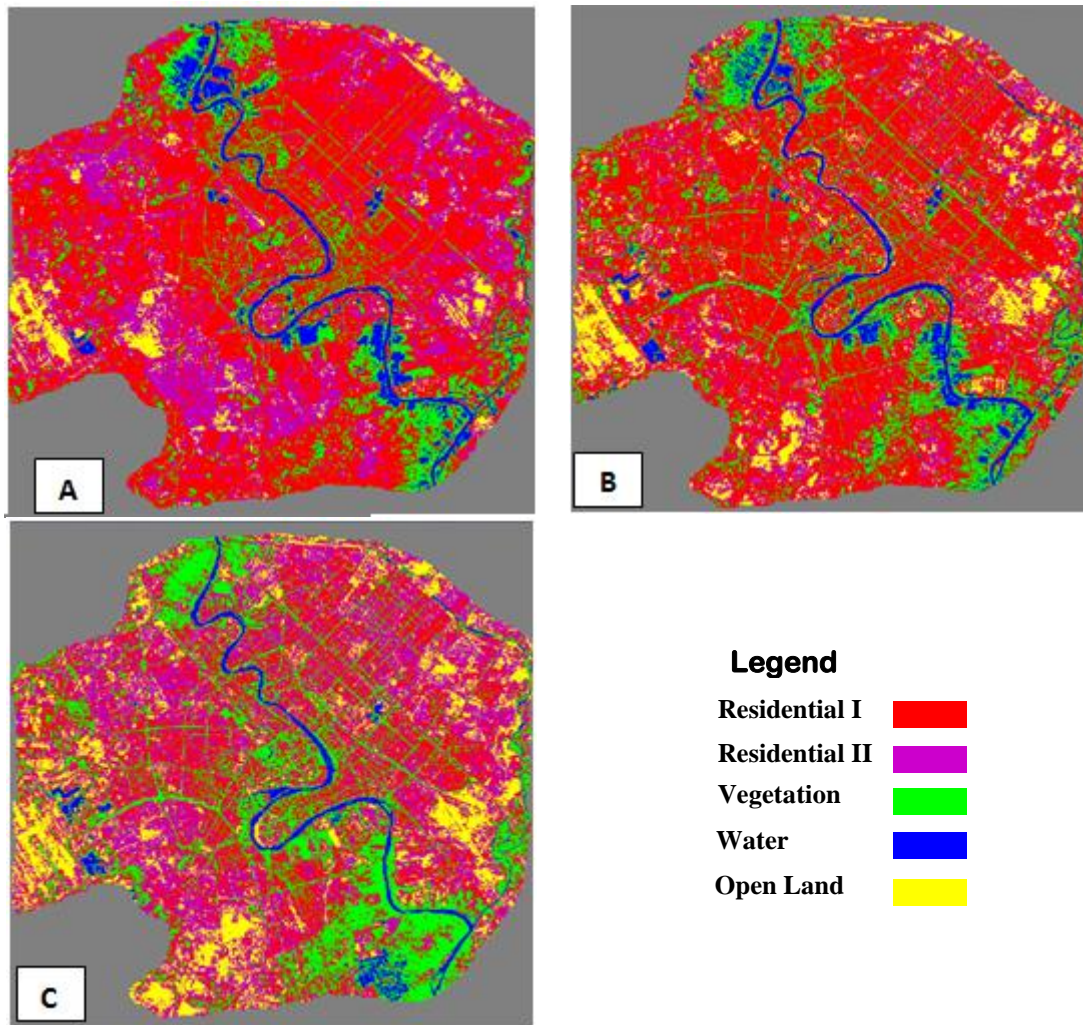


**Figure 8-** Results of supervised classification using singular value decomposition (SVD) algorithm (A) Landsat- 5 (TM) satellite image (27/8/1984), (B) Landsat- 7 (ETM+) satellite image (31/8/2000) (C) Landsat- 8 (OLI) satellite image (1/8/2015)

**Table 1-** Results of supervised classification statistics for all three Landsat satellite images using SVD algorithm

| CLASS NAME     | CLASS COLOR | Landsat-5 TM (1984)     |             | Landsat-7 ETM+ (2000)   |             | Landsat-8 OLI (2015)    |             |
|----------------|-------------|-------------------------|-------------|-------------------------|-------------|-------------------------|-------------|
|                |             | Area (KM <sup>2</sup> ) | Percent %   | Area (KM <sup>2</sup> ) | Percent %   | Area (KM <sup>2</sup> ) | Percent %   |
| Water          | Blue        | 13.166586               | 1.8629      | 14.6677846              | 2.0753      | 20.1940896              | 2.8572      |
| Vegetation     | Green       | 70.4906036              | 9.9735      | 142.978565              | 20.2296     | 131.733004              | 18.6385     |
| Residential I  | Red         | 256.95516               | 36.3558     | 249.213103              | 35.2604     | 288.739718              | 40.8529     |
| Residential II | Magenta     | 317.922623              | 44.9819     | 199.812078              | 28.2708     | 186.534527              | 26.3922     |
| Open Land      | Yellow      | 48.244027               | 6.8259      | 100.107471              | 14.1639     | 79.5776612              | 11.2592     |
| <b>Total</b>   |             | <b>706.7789996</b>      | <b>100%</b> | <b>706.7790016</b>      | <b>100%</b> | <b>706.7789998</b>      | <b>100%</b> |

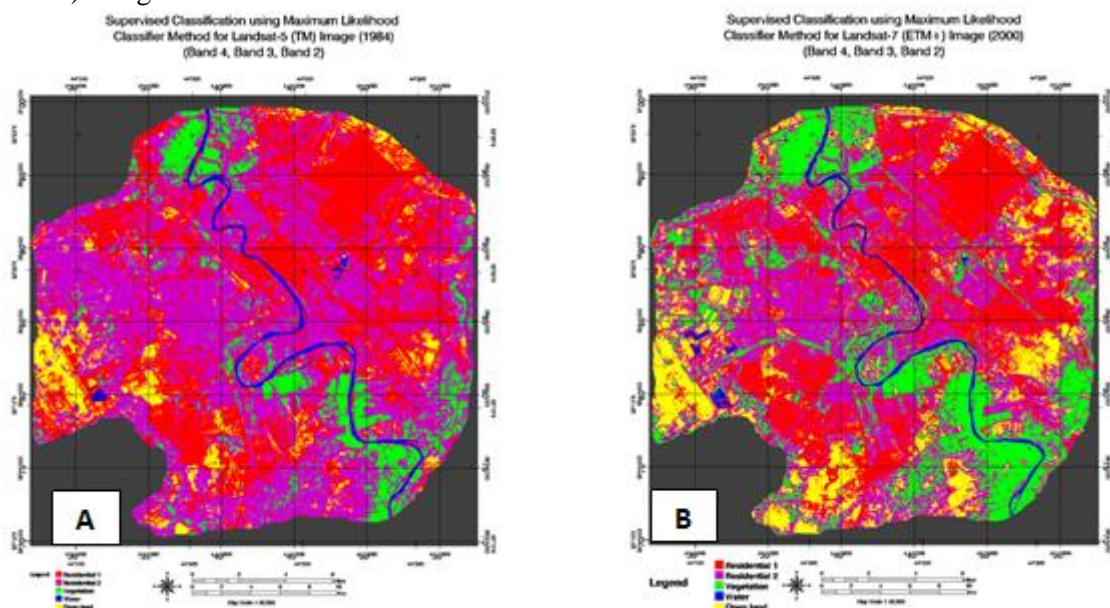
**5. Satellite Image Classification using Envi 5.1 Software:**

The methodology adopted for this stage including different image techniques; geometric correction, radiometric correction, atmospheric correction, false color composite (bands 4, 3 and 2) and image enhancement. Supervised classification was used in satellite image classification process. The algorithm used in supervised classification was the maximum likelihood classifier method to produce the land cover maps from Landsat TM, ETM+, and OLI satellite images for years 1984, 2000 and 2015. The block diagram of the methodology is shown in Figure-9.



**Figure 9-** Block Diagram of Methodology Using ENVI 5.1 Software

The training area collected from all imageries by selecting the region of interest (ROIs) using Envi software, the study area classified into five classes (residential I, residential II, vegetation, open land and water bodies). therefore, five ROIs were collected for Landsat images. Figure-10 shows the results of supervised classification for Landsat (TM, ETM+ and OLI) satellite images using maximum likelihood classifier method. The image classification of the study area resulted into five land cover types. Table-2 show the results of supervised classification statistics for all three years (1984, 2000 and 2015) using maximum likelihood classifier method.





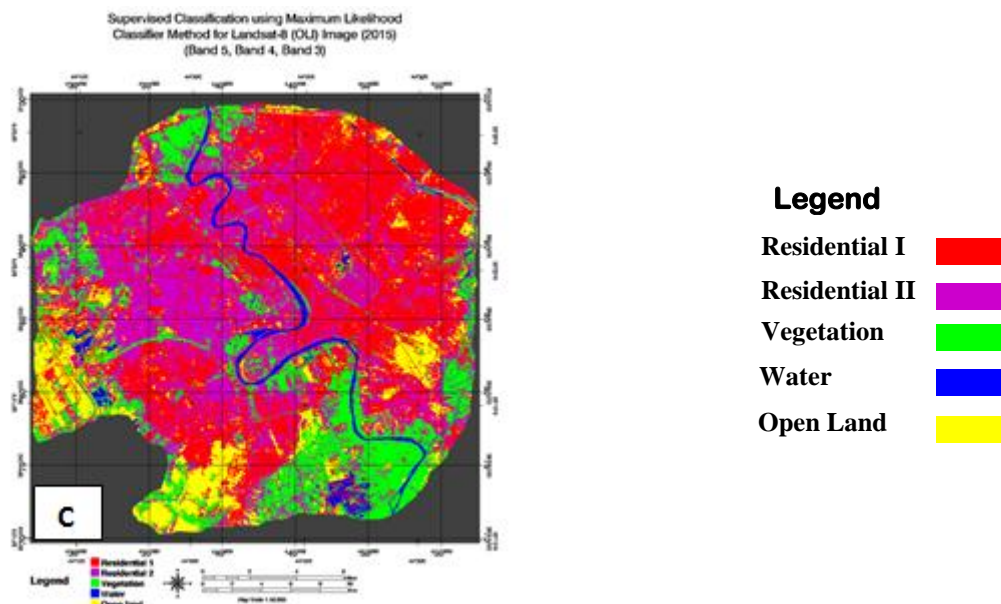


**Figure 10-** Results of supervised classification using maximum likelihood classifier method  
 (A) Landsat- 5 (TM) satellite image (27/8/1984), (B) Landsat- 7 (ETM+) satellite image (31/8/2000)  
 (C) Landsat- 8 (OLI) satellite image (1/8/2015)

**Table 2-**Results of supervised classification statistics for all three Landsat satellite images using Maximum Likelihood method

| CLASS NAME     | CLASS COLOR | Landsat-5 TM (1984)     |             | Landsat-7 ETM+ (2000)   |             | Landsat-8 OLI (2015)    |             |
|----------------|-------------|-------------------------|-------------|-------------------------|-------------|-------------------------|-------------|
|                |             | Area (KM <sup>2</sup> ) | Percent %   | Area (KM <sup>2</sup> ) | Percent %   | Area (KM <sup>2</sup> ) | Percent %   |
| Water          | Blue        | 12.636                  | 1.787829    | 12.4146                 | 1.756504    | 19.7073                 | 2.788326    |
| Vegetation     | Green       | 63.8127                 | 9.028664    | 134.8038                | 19.072978   | 126.2628                | 17.864538   |
| Residential I  | Red         | 251.2566                | 35.549528   | 223.5699                | 31.632222   | 274.7979                | 38.880315   |
| Residential II | Magenta     | 335.1609                | 47.420891   | 241.6968                | 34.196941   | 212.1552                | 30.017191   |
| Open Land      | Yellow      | 43.9128                 | 6.213088    | 94.2939                 | 13.341356   | 73.8558                 | 10.449631   |
| <b>Total</b>   |             | <b>706.779</b>          | <b>100%</b> | <b>706.779</b>          | <b>100%</b> | <b>706.779</b>          | <b>100%</b> |

### 6. Land Cover Change Detection:

In our work, monitoring land cover changes was achieved using three Landsat satellite images taken at different times represented by three dates; 1984, 2000 and 2015. The changes in land cover occurred in the study area in the period from 1984 to 2015 have been calculated by the subtraction processes. The results or the changes in land cover are illustrated in Tables-3 and 4 for SVD classification method. While, Tables 5 and 6 show the results of changes in land cover for maximum likelihood classifier method. Where the changes are given in square kilometers and in percent. The type of change (decrease or increase) is also shown.

**Table 3-**Changes in the Land Cover of the Period from 1984 to 2000 for Baghdad city using SVD Classification algorithm

| CLASS NAME     | Landsat-5 TM (1984)     |           | Landsat-7 ETM+ (2000)   |           | Relative Changes for Area (KM <sup>2</sup> ) | (2000-1984) Relative Changes % | Type of Change in Area |
|----------------|-------------------------|-----------|-------------------------|-----------|--|--------------------------------|------------------------|
|                | Area (KM <sup>2</sup> ) | Percent % | Area (KM <sup>2</sup> ) | Percent % |  |                                |                        |
| Water          | 13.166586               | 1.8629%   | 14.6677846              | 2.0753%   | 1.5011986                                    | 11.40%                         | increase               |
| Vegetation     | 70.4906036              | 9.9735%   | 142.978565              | 20.2296%  | 72.4879614                                   | 102.83%                        | increase               |
| Residential I  | 256.95516               | 36.3558%  | 249.213103              | 35.2604%  | -7.742057                                    | -3.01%                         | decrease               |
| Residential II | 317.922623              | 44.9819%  | 199.812078              | 28.2708%  | -118.110545                                  | -37.15%                        | decrease               |
| Open Land      | 48.244027               | 6.8259%   | 100.107471              | 14.1639%  | 51.863444                                    | 107.50%                        | increase               |

**Table 4-**Changes in the Land Cover of the Period from 1984 to 2015 for Baghdad city using SVD Classification algorithm

| CLASS NAME     | Landsat-5 TM (1984)     |           | Landsat-8 OLI (2015)    |           | Relative Changes for Area (km <sup>2</sup> ) | (2015-1984) Relative Changes % | Type of Change in Area |
|----------------|-------------------------|-----------|-------------------------|-----------|--|--------------------------------|------------------------|
|                | Area (km <sup>2</sup> ) | Percent % | Area (km <sup>2</sup> ) | Percent % |  |                                |                        |
| Water          | 13.166586               | 1.8629%   | 20.1940896              | 2.8572%   | 7.0275036                                    | 53.37 %                        | increase               |
| Vegetation     | 70.4906036              | 9.9735%   | 131.733004              | 18.6385%  | 61.2424004                                   | 86.88 %                        | increase               |
| Residential I  | 256.95516               | 36.3558%  | 288.739718              | 40.8529%  | 31.784558                                    | 12.36 %                        | increase               |
| Residential II | 317.922623              | 44.9819%  | 186.534527              | 26.3922%  | -131.388096                                  | -41.32 %                       | decrease               |
| Open Land      | 48.244027               | 6.8259%   | 79.5776612              | 11.2592%  | 31.3336342                                   | 64.94 %                        | increase               |

**Table 5-** Changes in the Land Cover of the Period from 1984 to 2000 for Baghdad city using Maximum Likelihood Classifier Method

| CLASS NAME     | Landsat-5 TM (1984)     |            | Landsat-7 ETM+ (2000)   |            | Relative Changes for Area (km <sup>2</sup> ) | (2000-1984) Relative Changes % | Type of Change in Area |
|----------------|-------------------------|------------|-------------------------|------------|--|--------------------------------|------------------------|
|                | Area (km <sup>2</sup> ) | Percent %  | Area (km <sup>2</sup> ) | Percent %  |  |                                |                        |
| Water          | 12.636                  | 1.787829%  | 12.4146                 | 1.756504%  | -0.2214                                      | -1.75 %                        | decrease               |
| Vegetation     | 63.8127                 | 9.028664%  | 134.8038                | 19.072978% | 70.9911                                      | 111.24 %                       | increase               |
| Residential I  | 251.2566                | 35.549528% | 223.5699                | 31.632222% | -27.6867                                     | -11.01 %                       | decrease               |
| Residential II | 335.1609                | 47.420891% | 241.6968                | 34.196941% | -93.4641                                     | -27.88 %                       | decrease               |
| Open Land      | 43.9128                 | 6.213088%  | 94.2939                 | 13.341356% | 50.3811                                      | 114.72 %                       | increase               |

**Table 6-** Changes in the Land Cover of the Period from 1984 to 2015 for Baghdad city using Maximum Likelihood Classifier Method

| CLASS NAME     | Landsat-5 TM (1984)     |            | Landsat-8 OLI (2015)    |            | Relative Changes for Area (km <sup>2</sup> ) | (2015-1984) Relative Changes % | Type of Change in Area |
|----------------|-------------------------|------------|-------------------------|------------|--|--------------------------------|------------------------|
|                | Area (km <sup>2</sup> ) | Percent %  | Area (km <sup>2</sup> ) | Percent %  |  |                                |                        |
| Water          | 12.636                  | 1.787829%  | 19.7073                 | 2.788326%  | 7.0713                                       | 55.96 %                        | increase               |
| Vegetation     | 63.8127                 | 9.028664%  | 126.2628                | 17.864538% | 62.4501                                      | 97.86 %                        | increase               |
| Residential I  | 251.2566                | 35.549528% | 274.7979                | 38.880315% | 23.5413                                      | 9.36 %                         | increase               |
| Residential II | 335.1609                | 47.420891% | 212.1552                | 30.017191% | -123.0057                                    | -36.70 %                       | decrease               |
| Open Land      | 43.9128                 | 6.213088%  | 73.8558                 | 10.449631% | 29.943                                       | 68.18 %                        | increase               |

From classification results using (SVD and maximum likelihood algorithms), the present study allows estimating the amount of significant land cover changes occurred at the study area during the two periods. The most significant change for the period 1984-2015 is represented by increasing the water body, area of vegetation, open land and urban area "residential I" (positive change), while, the change was negative represented by decrease of urban area "residential II".

The results from applying SVD classification method showed that the water, vegetation area, residential I and open land are in increase, water increased about 53.37%, vegetation area about 86.88%, "residential I" about 12.36% and finally open land increased about 64.94% in 2015 comparable with 1984, while, the second type from urban area "residential II" in decrease, about 41.32% in 2015 comparable with 1984. The results from applying maximum likelihood classifier method showed that the water, vegetation area, residential I and open land are in increase, water increased about 55.96%, vegetation area about 97.86%, "residential I" about 9.36% and finally open land increased about 68.18% in 2015 comparable with 1984, while, the second type from urban area "residential II" in decrease, about 36.7% in 2015 comparable with 1984.

### 7. Classification Accuracy Assessment:

Accuracy assessment is a procedure for quantifying how good a job was done by a classifier or how accurate out classification is. Accuracy assessment is an important part of classification. It is usually done by comparing the classification product with some reference data that is believed to reflect the true land cover accurately [12]. Sources of reference data include ground truth, higher spatial resolution images, and maps refer to Google map or Google Earth as needed. Assessing of the

final classification results has been performed manually on a field basis. In our work, number of random points have been chosen on each of classified images. These points compared with reference points. The results of accuracy assessment for all classification methods (SVD and maximum likelihood methods) are shown in Table-7.

**Table 7-** Accuracy Assessment Results

| Classification Type                      | Satellite Image  | Year | Accuracy Assessment (%) |
|--|------------------|------|-------------------------|
| SVD Classification Method                | Landsat-5 (TM)   | 1984 | 81%                     |
|  | Landsat-7 (ETM+) | 2000 | 78%                     |
|  | Landsat-8 (OLI)  | 2015 | 80%                     |
| Maximum Likelihood Classification Method | Landsat-5 (TM)   | 1984 | 90%                     |
|  | Landsat-7 (ETM+) | 2000 | 88%                     |
|  | Landsat-8 (OLI)  | 2015 | 91%                     |

## 8. Conclusions:

The basic idea of our work is to classify Landsat satellite images at different times for the study area using several methods and then compare the results of each method. From the results obtained, the following points are chosen for the present conclusions:

1. The study showed that the first factor of PCA bands often contain the majority of information residing in the original multi spectral Landsat images and can be used for more effective and accurate analyses because the number of image bands and the amount of image noises are reduced.
2. The first PCA layer is responsible for more than 95% of the total variation for each satellite image (95.8387%, 96.2976% and 99.1282% of the total variance for 1984, 2000 and 2015 Landsat images respectively). Therefore, the first principle component is suitable for classifying the multiband satellite images because, its contain the most ground information in study area and can be used to compare the changes in land cover classes in different years.
3. The primary stage of partitioning was accurately segmenting the image depending on the spectral uniformity, such that the founded block size differs from region to another in the image depending on the details found in that region. Therefore, the partitioning mechanisms using quad tree method produce small blocks when it contains high details, while the large blocks are produced if low details exit within the block.
4. The use of singular value decomposition algorithms was successfully determining the number of classes in the satellite image and showed good classification results. The classification accuracy for the proposed method singular value decomposition are 81%, 78% and 80% for years 1984, 2000 and 2015 respectively.
5. This research demonstrated the interest and efficiency of proposed method (PCA-transform, quad tree technique and singular value decomposition algorithm) as tools for detecting and monitoring changes of land cover processes of multi-spectral analysis with all spectral bands for different temporal intervals of satellite images.
6. Some factors such as selection of suitable change detection approach, suitable band and optimal threshold, may affect the success and accuracy of the classification.
7. Land cover dynamics is a result of complex interactions between human activities and natural factors. The effects of human activities are immediate and often radical, while the natural effects take a relatively longer period of time.
8. The results from classification process for study area indicated that water body, vegetation, open land and the first type from urban area "Residential I" are in increase (positive land cover change), while the second type from urban area "Residential II" in decrease (negative land cover change) for year 2015; comparable with 1984.

## 9. References:

1. Perumal, K. and Bhaskaran, R. **2010**. Supervised Classification Performance Multispectral Images, *Journal of Computing* ,2, pp:124-129.
2. Anand, U., Santosh, K. S. and Vipin, G.S. **2014**. Impact of features on classification accuracy of IRS LISS-III images using artificial neural network, *International Journal of Application Innovation in Engineering and Management*, 3, pp:311-317.



3. Mamdouh, M. Abdeen and Fatima Al Masoudi. Utilization of Multi-Dates and Multi-Sensors Remote Sensing Data in Monitoring Land Use/Land Cover Changes in Kuwait, Geography Department, Kuwait University, Alshuwaykh, State of Kuwait.
4. Paul M. Mather, and Magaly, K. **2011**. *Computer Processing of Remotely-Sensed Images: An Introduction*, Wiley Blackwell, Nottingham, Fourth Edition.
5. M. Anji Reddy. **2008**. *Textbook of Remote Sensing and Geographical Information Systems*, BS Publications, Third Edition.
6. Ravi P. Gupta, Reet K. Tiwari, Varinder Saini and Neeraj Srivastava. **2013**. A Simplified Approach for Interpreting Principal Component Images. *Advances in Remote Sensing*, 2, pp:111-119.
7. Balaji T. and Sumathi M. **2014**. PCA Based Classification of Relational and Identical Features of Remote Sensing Images, *International Journal of Engineering and Computer Science*, 3(7), pp:7221-7228.
8. Bushra Qassim Al-Abudi. **2002**. Color Image Data Compression Using Multilevel Block Truncation Coding Technique, Ph.D. Thesis, Baghdad University, College of Science.
9. Chu Hui Lee and Kun-Cheng Chiang. **2010**. Latent Semantic Analysis for Classifying Scene Images, Proceedings of the International Multiconference of Engineers and Computer Scientists, Hong Kong, 2, pp:17-19.
10. Pavel, P., Libor, M. and Vaclav, S. **2004**. Iris Recognition Using the SVD-Free Latent Semantic Indexing", Fifth International Workshop on Multimedia Data Mining, pp:67-70.
11. Bhandari, A. K., Kumar, A. and Padhy, P. K. **2011**. Enhancement of Low Contrast Satellite Images using Discrete Cosine Transform and Singular Value Decomposition, *World Academy of Science, Engineering and Technology Journal* ,5, pp:20-26.
12. R. G. Congalton, and K. Green. **1999**. *Assessing the Accuracy of Remotely Sensed Data: Principles and Practices*, Lewis Publishers, Boca Raton.